REPORT DOCUMENTATION PAGE

Form Approved OMB NO. 0704-0188

1. REPORT DATE (DD-MM-YYYY)	2. REPORT TYPE	3. DATES COVERED (From - To)
	New Reprint	-

4. TITLE AND SUBTITLE

The effect of annealing on the photoconductivity of carbon nanofiber/TiO2core-shell nanowires for use in dye-sensitized solar cells

5a. CONTRACT NUMBER
W911NF-09-1-0295

5b. GRANT NUMBER

5c. PROGRAM ELEMENT NUMBER
611102

6. AUTHORS

Caitlin Rochford, Zhuangzhi Li, Javier Baca, Jianwei Liu, Jun Li, Judy Wu

5d. PROJECT NUMBER

5e. TASK NUMBER

5f. WORK UNIT NUMBER

7. PERFORMING ORGANIZATION NAMES AND ADDRESSES

University of Kansas Center for Research, Inc.
2385 Irving Hill Road

Lawrence, KS 66045 -7568

8. PERFORMING ORGANIZATION REPORT NUMBER

9. SPONSORING/MONITORING AGENCY NAME(S) AND ADDRESS(ES)

U.S. Army Research Office
P.O. Box 12211
Research Triangle Park, NC 27709-2211

10. SPONSOR/MONITOR'S ACRONYM(S)
ARO

11. SPONSOR/MONITOR'S REPORT NUMBER(S)
56050-EL.12

12. DISTRIBUTION AVAILIBILITY STATEMENT

Approved for public release; distribution is unlimited.

13. SUPPLEMENTARY NOTES

The views, opinions and/or findings contained in this report are those of the author(s) and should not contrued as an official Department of the Army position, policy or decision, unless so designated by other documentation.

14. ABSTRACT

Electrical transport properties and photoresponse of individual TiO2-coated carbon nanofibers were studied in an attempt to elucidate the limiting factors of core-shell nanowire-based dye-sensitized solar cells □DSSC□. The role of the semiconductor shell microstructure was investigated by comparing as grown and thermally annealed samples. Steady state I-V and transient photoconductivity measurements suggest that improving the microstructure leads to reduced

15. SUBJECT TERMS

photovoltaic, core-shell nanostructure, photoconductivity

16. SECURITY CLASSIFICATION OF:			17. LIMITATION OF ABSTRACT	15. NUMBER OF PAGES	19a. NAME OF RESPONSIBLE PERSON
a. REPORT	b. ABSTRACT	c. THIS PAGE			Judy Wu
UU	UU	UU	UU		19b. TELEPHONE NUMBER: 785-864-3240

Report Title

The effect of annealing on the photoconductivity of carbon nanofiber/TiO2core-shell nanowires for use in dye-sensitized solar cells

ABSTRACT

Electrical transport properties and photoresponse of individual TiO2-coated carbon nanofibers were studied in an attempt to elucidate the limiting factors of core-shell nanowire-based dye-sensitized solar cells □DSSC□. The role of the semiconductor shell microstructure was investigated by comparing as grown and thermally annealed samples. Steady state I-V and transient photoconductivity measurements suggest that improving the microstructure leads to reduced resistivity and contact resistance, a decrease in charge traps, improved surface stoichiometry for dye adsorption, and reduced absorption of visible light by the semiconductor, all of which may improve nanowire-based DSSC performance. ©

REPORT DOCUMENTATION PAGE (SF298)
(Continuation Sheet)

Continuation for Block 13

ARO Report Number 56050.12-EL
The effect of annealing on the photoconductivity ...

Block 13: Supplementary Note

Approved for public release; distribution is unlimited.

The effect of annealing on the photoconductivity of carbon nanofiber/TiO_2 core-shell nanowires for use in dye-sensitized solar cells

Caitlin Rochford,[1,a)] Zhuang-Zhi Li,[2] Javier Baca,[3] Jianwei Liu,[1] Jun Li,[4] and Judy Wu[1]
[1]*Department of Physics and Astronomy, University of Kansas, Lawrence, Kansas 66045, USA*
[2]*Department of Physics, Hebei Advanced Thin Film Laboratory, Hebei Normal University, Shijiazhuang 050016, People's Republic of China*
[3]*Los Alamos National Laboratory, Los Alamos, New Mexico 87545, USA*
[4]*Department of Chemistry, Kansas State University, Manhattan, Kansas 66506, USA*

(Received 17 May 2010; accepted 26 June 2010; published online 26 July 2010)

Electrical transport properties and photoresponse of individual TiO_2-coated carbon nanofibers were studied in an attempt to elucidate the limiting factors of core-shell nanowire-based dye-sensitized solar cells (DSSC). The role of the semiconductor shell microstructure was investigated by comparing as grown and thermally annealed samples. Steady state I-V and transient photoconductivity measurements suggest that improving the microstructure leads to reduced resistivity and contact resistance, a decrease in charge traps, improved surface stoichiometry for dye adsorption, and reduced absorption of visible light by the semiconductor, all of which may improve nanowire-based DSSC performance. © *2010 American Institute of Physics*.
[doi:10.1063/1.3464965]

In recent years semiconductor nanowires[1,2] (NWs) and nanotubes[3,4] (NTs) have been utilized in an attempt to improve electron transport and hence efficiency of dye-sensitized solar cells (DSSC) by providing electrons with a highly conductive, direct route to the anode. This is in contrast to the traditionally used mesoporous TiO_2 film in which the injected electrons must travel through an average of 10^6 nanoparticles in order to be collected.[5] In contrast, while NW and NT arrays may offer a lower specific surface area than the nanoparticle film, they are commonly found to have a superior electron lifetime and diffusion length and may allow the formation of a depletion layer to separate electrons from oxidizing species. Additionally, NT or NW geometry also provides enhanced light scattering[3] which may improve absorption of long wavelength light.

The superiority of crystalline NWs over nanoparticles is clearly demonstrated in the influential work by Law *et al.* in which the first ordered NW-based DSSC was reported to have an efficiency of 1.5%. The authors attributed the low efficiency to the limited roughness factor of 200, compared to 1000 for nanoparticle DSSCs.[1] Exceeding the current DSSC efficiency of over 10% (Ref. 6) using a NW-based design thus depends critically on increasing surface area for dye adsorption. One way to achieve this is through use of core-shell nanostructures which employ a conductive core and a rough semiconductor shell.[7,8] One such design, based upon a vertically aligned carbon nanofiber (CNF) array coated with nanoneedle textured TiO_2, was recently reported by Liu *et al.*[7] The nanoneedle structure offers an enhanced TiO_2 surface area for dye adsorption compared to bare NWs. Additionally, the CNF core allows for efficient electron transport, and the core-shell structure spatially separates the electrons from the oxidized species in the electrolyte and oxidized dye molecules. The energy conversion efficiency of the CNF/TiO_2 core-shell NW-based DSSC was reported to be 1.09%. Despite the potential advantages, this device, along with other core-shell DSSCs, is so far unable to offer a significant improvement over single crystal NWs. Systematic studies of these core-shell units are thus needed in order to elucidate the caveats of their use and determine an optimal structure.

In this work we utilize a single NW approach to study the role of the semiconductor microstructure as related to DSSC performance using CNF/TiO_2 NWs. Analysis of two sets of NWs is presented, one of which underwent an annealing treatment in air to improve the structural order. As a first simplifying step, we have chosen to study NWs which have formed a complete TiO_2 shell but have not yet produced the full nanoneedle structure utilized in the reported DSSC. This way the focus will be on transport through the TiO_2 and not between nanoneedles since the nature of their electrical connection is unknown at this time but will be a subject of future research.

The details of the growth are described elsewhere.[9] An extra annealing treatment was applied to half of the samples for 30 min at 400 °C in air. While annealing at a slightly higher temperature in air has been shown to induce crystal grain growth in TiO_2 NTs,[10] a lower temperature of 400 °C was chosen to avoid damage to the CNF in the air. The NWs were dispersed into ethanol and drop cast onto Si substrate with 500 nm thermal SiO_2. Electron beam lithography was used to pattern two to four electrodes. Before Ti (15 nm)/Au (150 nm) electrode deposition, the contact surfaces were treated with O_2 plasma at 20 W for 30 s via reactive ion etching to remove residual organic contaminants and obtain Ohmic contact. Finally, all samples were annealed at 400 °C for 30 min at $\sim 10^{-6}$ Torr. This annealing step, performed in vacuum in order to avoid oxidation of Ti in the bottom layer of the electrode, serves to both improve contact resistance and desorb possible residual chemicals on the surface of the NWs due to the above processes. The microstructure of the NWs was characterized using high resolution transmission

a)Electronic mail: caitlinr@ku.edu.

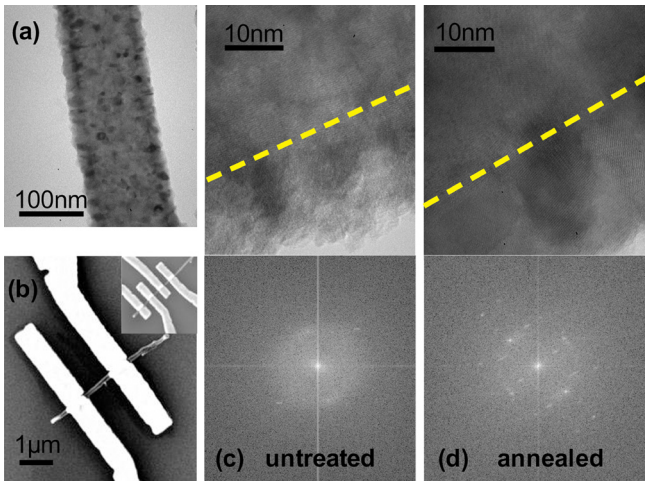

FIG. 1. (Color online) (a) TEM image of CNF/TiO_2 nanowire used in this study, inset shows a nanowire prepared for four-probe measurements, (b) scanning electron micrograph image of a two probe CNF/TiO_2 single nanowire device, [(c) and (d)] high resolution TEM images (top) and FFT (bottom) of an untreated and annealed nanowire showing the difference in crystalline order. The location of the interface between the CNF core and TiO_2 shell in the TEM image is marked with a dashed line.

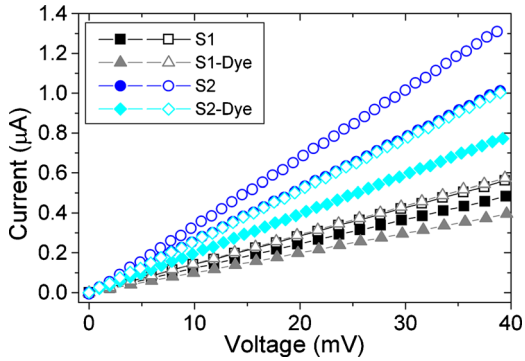

FIG. 2. (Color online) Dark (solid markers) and 1 sun (open markers) I-V curves for S1 (squares, triangles) and S2 (circles, diamonds) with and without dye (respectively).

electron microscopy (HRTEM) with fast Fourier Transform (FFT). The I-V characteristics and transient response to light were measured using a Keithley 6487 picoammeter/voltage source. Before dark measurements the samples were allowed to sit in the dark for 16 h in order to allow the photoconductivity to decay. To attach dye, samples were soaked in 0.2 mM ethanol solution of N719 dye (Solaronix) for 12 h. Simulated sunlight was provided by a 300 W ozone free Xenon lamp with collimated output (Newport 67005) and AM 1.5 G filter.

Figure 1(a) shows a TEM image of a typical CNF/TiO_2 NW. The average diameter of the CNF was found to be approximately 100 nm and the TiO_2 shell 20–25 nm thick. Figure 1(b) shows a typical scanning electron micrograph of a single CNF/TiO_2 nanowire device prepared for two probe and (inset) four probe measurements. Figures 1(c) and 1(d) show a representative HRTEM image and corresponding FFT, respectively, for unannealed and annealed NWs used in this study. The location of the interface between the core and shell is marked with a dashed line for clarity. In the top halves of Figs. 1(c) and 1(d) the annealed sample appears to contain larger crystallites (10–15 nm) with distinct ordered planes while the untreated sample appears to contain smaller crystallites (5–9 nm) within an amorphous phase. The bottom halves of Figs. 1(c) and 1(d) show FFT of the images and illustrate the change in overall crystalline order. The FFT of the untreated sample exhibits continuous rings and a weak pattern of discrete spots, indicating the presence of amorphous TiO_2 and some fine crystallites. The annealed sample exhibits multiple sets of discrete spots, indicative of the observed larger single crystal TiO_2 grains. A close examination of Fig. 1(d) suggests that these single crystal grains form a continuous layer around the CNF core.

Data from two representative samples are presented in this paper, although more than ten samples were investigated. S1 is the untreated sample, and S2 is the annealed sample. Dark and illuminated I-V characteristics of both samples with and without dye are shown in Fig. 2. Based on four probe measurements, the resistivity was found to be 10^{-1}–10^{-2} Ω cm for the untreated samples 10^{-2}–10^{-3} Ω cm for the annealed samples. These values lie between the reported ranges for a bare CNF (10^{-3} Ω cm)[11] and anatase TiO_2 thin films (10^{-1}–10^{6} Ω cm).[12,13] Reduction of CNF resistivity after annealing is not expected since chemical reactions that may occur involving the carbon atoms typically lead to higher resistivity compounds. The drop in resistivity is therefore attributed to the improved TiO_2 structural order, as follows. The unannealed sample contains nanoscale crystallites embedded in amorphous TiO_2, the resistance of the former being several orders of magnitude lower than the latter,[14] so that charges must hop between crystallites. The enhanced TiO_2 crystallite size may facilitate such "hopping" dominated charge transport by reducing or eliminating the amorphous gap between the crystallites.

As can be seen in Fig. 2, both devices exhibit a significant dark conductance, generally accepted to be due to n-type doping caused by oxygen vacancies in TiO_2. Without dye, the dark resistance of S1 is approximately twice that of S2, which is likely due to the improved charge transport in the more ordered TiO_2 layer of S2. Additionally, individual CNFs were found to exhibit no photoresponse under the reported conditions, so any response is assumed to be due to TiO_2 only. Without dye, the illuminated current is 17% higher than the dark for S1 and 30% higher for S2. The cause of the large photo-induced current, defined as the difference between illuminated and dark currents, for both samples has two main components: subband gap absorption due to localized defect states within the bandgap[15] and photoconductivity due to hole trapping in the TiO_2 shell, which can be explained by a simple model proposed by Sheinkman and Shik.[16] The larger photo-induced current observed for S2 suggests that a larger volume portion of crystalline TiO_2 leads to more efficient charge transport of photo-excited electrons.

Figure 2 also shows the dark and illuminated I-V characteristics of both samples after dye attachment. The dark conductivity is decreased after dye attachment for both S1 and S2. This is likely due to the passivation of hole traps during dye attachment, particularly by protons which previously resided on the carboxyl group of the N719 dye before it became bound to TiO_2. It can be seen that the photo-induced current is increased for S1 while it remains essentially constant for S2. It should be noted that the dye is unable to contribute directly to the current due to the absence of the electrolyte, and so the difference must be attributed primarily to conductivity, specifically free electron density.

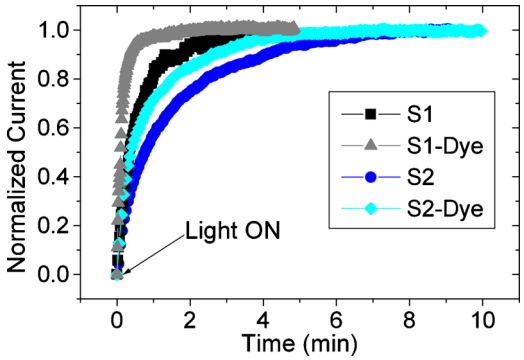

FIG. 3. (Color online) Normalized photoinduced current onset at 100 mV for S1 (squares, triangles) and S2 (circles, diamonds) with and without dye (respectively).

Molecular oxygen is a known electron scavenger on the surface of TiO_2,[17] and the presence of dye molecules may be able to block the adsorption of molecular oxygen and the subsequent scavenging of conduction electrons to form O_2^- sites. During the annealing of S2, however, molecular oxygen can dissociate and fill oxygen vacancies on the surface and diffuse into subsurface regions. Since oxygen vacancies can act as active sites for chemisorption of molecular oxygen,[18] electron scavenging may already be minimized in S2 before dye is attached due to its improved surface stoichiometry. This is supported by work by Pan *et al.*, which found that oxygen did not adsorb on stoichiometric TiO_2 surfaces.[19]

As previously mentioned, the samples exhibit transient photoconductivity, a well documented phenomenon in nanocrystalline TiO_2 thin films.[15] As can be seen in Fig. 3, the current increases sharply after the onset of illumination and then levels off. Fitting the data to a simple exponential function results in time constants of 0.59 and 0.14 min for S1 and 1.4 and 0.75 min for S2 without and with dye, respectively. These differences are significantly larger than the observed sample to sample variability of a few seconds. The slow response is due to electron trapping via hydroxylated Ti sites on the surface and electron scavenging by oxygen molecules in the surrounding atmosphere.[17] A steady state current cannot be achieved until equilibrium is established between these events and their corresponding reverse processes. Since both measurements on S1 and S2 were made under the same conditions, the difference in rise times without dye could be attributed to a lower oxygen adsorption rate in S2 due to its improved surface stoichiometry. It can also be seen that both samples experience a decrease in rise time with dye. This is likely due to the lower number of hydroxylated Ti sites and electron scavenging events on the surface due to dye attachment. Further, the drop in rise time is more drastic for S1, which supports the argument that the surface stoichiometry is improved in the annealed sample. A corresponding trend was observed in the photoconductivity decay times (not shown). The decay time, which depends on electron-hole recombination at hole traps, decreased after annealing and again after dye attachment for both samples. This supports the claims that annealing in air can decrease the number of oxygen vacancies and that dye attachment passivates hole traps. Kim *et al.*[20] found that reducing the number of oxygen vacancies on the surface of TiO_2 increased the amount of adsorbed N719 dye, which was explained by an increased electrostatic interaction between the $-COO^-$ groups of the dye and the Ti^{4+} sites on the treated surface compared to the Ti^{3+} sites on the surface with more oxygen vacancies. Therefore, taking steps to decrease the number of oxygen vacancies on the surface of the NWs could lead to a higher dye loading and thus higher photocurrent and efficiency.

In conclusion, the effect of annealing on the conductivity of single CNF/TiO_2 core-shell NWs was studied in an attempt to elucidate the limiting factors of the CNF/TiO_2 NW array-based DSSC and motivate design constraints for future core-shell nanostructure-based DSSCs. The NWs which underwent an annealing treatment in air contained larger crystallites and much reduced amorphous TiO_2, which decreased the nanowire resistivity and increased photoconductivity. Further, since amorphous TiO_2 may not be able to effectively transport electrons to the CNF due to its high resistivity, any dye molecules adsorbed on the amorphous phase may be unable to contribute significantly to the DSSC photocurrent. The transient measurements suggest that the number of oxygen vacancies, which act as band gap states and hole traps, is reduced in the annealed sample. This is beneficial for DSSC performance since it may increase the dye loading and also decrease the absorption of visible light by TiO_2.

C.R. acknowledges a NSF Graduate Research Fellowship. The authors acknowledge support from NSF EPSCoR for this work. J.W. was also supported in part by ARO (contract No. ARO-W911NF-09–1–0295) and NSF (contract Nos. NSF-DMR-0803149 and NSF EPSCoR-0903806), and matching support from the State of Kansas through Kansas Technology Enterprise Corporation.

[1]M. Law, L. E. Greene, J. C. Johnson, R. Saykally, and P. Yang, Nature Mater. **4**, 455 (2005).
[2]B. Tan and Y. Wu, J. Phys. Chem. B **110**, 15932 (2006).
[3]K. Zhu, N. Neale, A. Miedaner, and A. Frank, Nano Lett. **7**, 69 (2007).
[4]G. K. Mor, K. Shankar, M. Paulose, O. K. Varghese, and C. A. Grimes, Nano Lett. **6**, 215 (2006).
[5]K. D. Benkstein, N. Kopidakis, J. van de Lagemaat, and A. J. Frank, J. Phys. Chem. B **107**, 7759 (2003).
[6]M. Grätzel, Nature (London) **414**, 338 (2001).
[7]J. Liu, Y. Kuo, K. J. Klabunde, C. Rochford, J. Wu, and J. Li, ACS Applied Materials & Interfaces **1**, 1645 (2009).
[8]Z. Yang, T. Xu, Y. Ito, U. Welp, and W. K. Kwok, J. Phys. Chem. C **113**, 20521 (2009).
[9]J. Liu, J. Li, A. Sedhain, J. Lin, and H. Jiang, J. Phys. Chem. C **112**, 17127 (2008).
[10]A. Ghicov, H. Tsuchiya, J. M. Macak, and P. Schmuki, Phys. Status Solidi A **203**, R28 (2006).
[11]L. Zhang, D. Austin, V. I. Merkulov, A. V. Meleshko, K. L. Klein, M. A. Guillorn, D. H. Lowndes, and M. L. Simpson, Appl. Phys. Lett. **84**, 3972 (2004).
[12]T. Miyata, S. Tsukada, and T. Minami, Thin Solid Films **496**, 136 (2006).
[13]R. Könenkamp, A. Wahi, and P. Hoyer, Thin Solid Films **246**, 13 (1994).
[14]P. Kern, R. Widmer, P. Gasser, and J. Michler, J. Phys. Chem. C **111**, 13972 (2007).
[15]D. Comedi, S. P. Heluani, M. Villafuerte, R. D. Arce, and R. R. Koropecki, J. Phys. Condens. Matter **19**, 486205 (2007).
[16]M. K. Sheinkman and A. Ya. Shik, Sov. Phys. Semicond. **10**, 128 (1976).
[17]S. H. Szczepankiewicz, A. J. Colussi, and M. R. Hoffmann, J. Phys. Chem. B **104**, 9842 (2000).
[18]W. Göpel, G. Rocker, and R. Feierabend, Phys. Rev. B **28**, 3427 (1983).
[19]J. Pan, B. L. Maschhoff, U. Diebold, and T. E. Madey, J. Vac. Sci. Technol. A **10**, 2470 (1992).
[20]Y. Kim, B. J. Yoo, R. Vittal, Y. Lee, N. G. Park, and K. J. Kim, J. Power Sources **175**, 914 (2008).